This article was downloaded by: [Renmin University of China]
On: 13 October 2013, At: 10:20
Publisher: Taylor & Francis
Informa Ltd Registered in England and Wales Registered Number: 1072954 Registered office: Mortimer House, 37-41 Mortimer Street, London W1T 3JH, UK

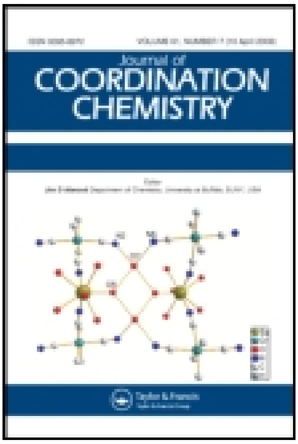

Journal of Coordination Chemistry
Publication details, including instructions for authors and subscription information:
http://www.tandfonline.com/loi/gcoo20

Synthesis, spectral, bioactivity, and NLO properties of chalcone metal complexes

S. Sumathi [a], P. Tharmaraj [a], C.D. Sheela [b] & R. Ebenezer [a]
[a] Department of Chemistry, Thiagarajar College, Madurai-625 009, India
[b] Department of Chemistry, The American College, Madurai-625 002, India

Published online: 11 May 2011.

To cite this article: S. Sumathi, P. Tharmaraj, C.D. Sheela & R. Ebenezer (2011) Synthesis, spectral, bioactivity, and NLO properties of chalcone metal complexes, Journal of Coordination Chemistry, 64:10, 1707-1717, DOI: 10.1080/00958972.2011.580844

To link to this article: http://dx.doi.org/10.1080/00958972.2011.580844

PLEASE SCROLL DOWN FOR ARTICLE

Taylor & Francis makes every effort to ensure the accuracy of all the information (the "Content") contained in the publications on our platform. However, Taylor & Francis, our agents, and our licensors make no representations or warranties whatsoever as to the accuracy, completeness, or suitability for any purpose of the Content. Any opinions and views expressed in this publication are the opinions and views of the authors, and are not the views of or endorsed by Taylor & Francis. The accuracy of the Content should not be relied upon and should be independently verified with primary sources of information. Taylor and Francis shall not be liable for any losses, actions, claims, proceedings, demands, costs, expenses, damages, and other liabilities whatsoever or howsoever caused arising directly or indirectly in connection with, in relation to or arising out of the use of the Content.

This article may be used for research, teaching, and private study purposes. Any substantial or systematic reproduction, redistribution, reselling, loan, sub-licensing, systematic supply, or distribution in any form to anyone is expressly forbidden. Terms & Conditions of access and use can be found at http://www.tandfonline.com/page/terms-and-conditions

Journal of Coordination Chemistry
Vol. 64, No. 10, 20 May 2011, 1707–1717

Synthesis, spectral, bioactivity, and NLO properties of chalcone metal complexes

S. SUMATHI†, P. THARMARAJ*†, C.D. SHEELA‡ and R. EBENEZER†

†Department of Chemistry, Thiagarajar College, Madurai-625 009, India
‡Department of Chemistry, The American College, Madurai-625 002, India

(*Received 13 November 2010; in final form 18 March 2011*)

A series of metal(II) complexes ML and ML_2 [where M = Cu(II), Co(II), Ni(II), Zn(II), Mn(II), Cd(II), and VO(II); L = 2-hydroxyphenyl-3-(1H-indol-3-yl)-prop-2-en-1-one (HPIP)] have been prepared and characterized by elemental analysis, magnetic susceptibility, molar conductance, IR, UV-Vis, NMR, Mass, and ESR spectral studies. Conductivity measurements reveal that the complexes are non-electrolytes, except VO(II) complex. Spectroscopy and other data show square pyramidal geometry for oxovanadium and octahedral geometry for the other complexes. Redox behavior of the copper(II) and vanadyl complexes has been studied with cyclic voltammetry. Antimicrobial activities against several microorganisms indicate that a few complexes exhibit considerable activity. The nuclease activity shows that the complexes cleave DNA. All synthesized compounds can serve as potential photoactive materials as indicated from their characteristic fluorescence properties. The second harmonic generation efficiency of the ligand is higher than that of urea and KDP.

Keywords: 2-Hydroxyphenyl-3-(1H-indol-3-yl)-prop-2-en-1-one; Indole-3-aldehyde; Metal(II) complexes; DNA studies; Fluorescence; SHG

1. Introduction

Chalcones are open-chain flavonoids, in which the bichromophoric molecules are separated by a hetero-vinyl chain. They undergo a variety of chemical reactions and are useful in the synthesis of heterocyclic compounds. Chalcones have been used as intermediates for the preparation of compounds having therapeutic value. Such compounds exhibit wide spectrum behavior, such as biological activities [1–8], agrochemicals, drugs, azo dyes, interaction with nucleic acids [9–11]. The presence of indole nucleus is the key factor for various biocidal activities [12–14] and metal complexes of these systems have received considerable interaction in nucleic acid chemistry [15–17]. Such molecules also possess a variety of photochemical properties [18–20] and find optical applications in nonlinear optics (NLO), photorefractive polymers, fluorescent probes, etc. Hence, we synthesize chalcone, 2-hydroxyphenyl-3-(1H-indol-3-yl)-prop-2-en-1-one (HPIP) and study various properties. In this article,

---

*Corresponding author. Email: ptharma@rediffmail.com

Journal of Coordination Chemistry
ISSN 0095-8972 print/ISSN 1029-0389 online © 2011 Taylor & Francis
DOI: 10.1080/00958972.2011.580844

we present the characterization, biological screening, nonlinear optical property, fluorescence, and DNA activity of the ligand and metal complexes.

2. Experimental

All chemicals and solvents were purchased from commercial sources. o-Hydroxyacetophenone and indole-3-aldehyde were Merck India products and used as supplied. Solvents were doubly distilled and stored in molecular sieves (4Å) before use. For voltammetric experiments, tetrabutylammonium perchlorate (TBAP) (Sigma) was used as supporting electrolyte. NMR measurement was made on a BRUKER 300 MHz spectrometer (Madurai Kamaraj University, Madurai). Mass spectrum was performed in a VG 7070 H instrument (IICT, Hyderabad). UV-Vis spectra were obtained using a THERMO SPECTRONIC 6 HEXIOS α and fluorescence spectra were taken with an ELICO SL174 spectrofluorometer (Lady Doak College, Madurai) in DMSO. IR spectra were obtained on a SHIMADZU FTIR 8400 S (Standard Fire Work College, Sivakasi). ESR spectra of the copper(II) complexes were recorded at 300 and 77 K (IIT, Mumbai) using tetracyanoethylene (TCNE) as the g-marker. Magnetic susceptibilities of the complexes were measured on a Sherwood Magnetic susceptibility balance Mk1 (Thiagarajar College, Madurai). Cyclic voltammetric (CV) studies for Cu(II) and VO(II) complexes in DMSO were carried out on a CH Instruments (USA). Molar conductances of the complexes were measured in DMSO at room temperature using a Systronic Conductivity Bridge 304. All the complexes were screened for biological activity through the well diffusion method. The second harmonic generation (SHG) efficiency of HPIP was determined by the modified version of powder technique (IISc, Bangalore).

2.1. *Synthesis of HPIP*

A mixture of o-hydroxyacetophenone (1.36 g, 1 mmol) and indole-3-aldehyde (1.45 g, 1 mmol) in ethanol was refluxed by adding piperidine for a period of 48 h (figure 1). The solution was concentrated through rotavaporation and the resulting residue was refrigerated; the yellow solid obtained was filtered and recrystallized from ethanol. Yield: 80%, m.p.: 145°C [^{1}H-NMR, 13.25 δ (s, 1H, –OH), 8.721 δ (s, 1H, >NH), 6.91–8.21 δ (m, aromatic proton), 7.711, and 8.219 δ (d, 15.3 Hz, olefinic *trans* coupling protons); ^{13}C-NMR, 17 peaks corresponding to all carbons; mass spectra (Supplementary material), $[M]^+$ at 263 m/e and other ion peaks at 261, 196, 170, 143, 115, 65, and 39 m/e].

2.2. *Synthesis of metal(II) complexes*

2.2.1. Synthesis of [ML] complexes. A solution of metal(II) chloride (1 mmol) in ethanol was stirred with an ethanolic solution of HPIP (0.26 g, 1 mmol) on a magnetic stirrer at room temperature. Upon concentration, the precipitated solid was filtered and washed thoroughly with ethanol and dried in vacuum.

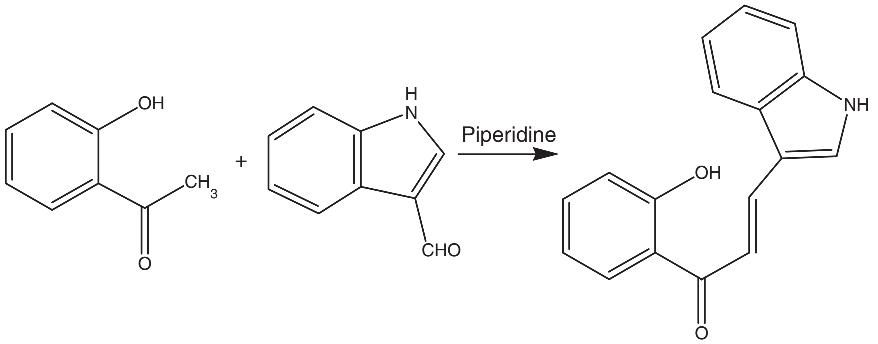

Figure 1. Synthesis of HPIP.

2.2.2. Synthesis of [ML2] complexes. A solution of metal(II) chloride (1 mmol) in ethanol was stirred with an ethanolic solution of HPIP (0.52 g, 2 mmol) on a magnetic stirrer at room temperature. The complex precipitated upon concentration was filtered, washed with ethanol, and dried in vacuum. The oxovanadium complex was synthesized from the ligand and oxovanadium sulfate by adopting the above method under reflux and concentrating the solution through rotavaporation.

2.3. *Nonlinear optical properties of HPIP*

The SHG efficiency of HPIP was determined by the modified version of the powder technique developed by Kurtz and Perry [21]. The ligand was ground into powder and packed between two transparent glass slides. A Nd : YAG laser beam of wavelength 1064 nm was passed through the sample cell. The transmitted fundamental wave was absorbed by a copper(II) sulfate solution, which removes the incident 1064 nm light and Filter BG-38 removing any residual 1064 nm light. Interference filter band width is 4 nm and for central wavelength of 532 nm. Green light is finally detected by the photomultiplier tube and displayed on the oscilloscope. The second harmonic signal was detected by a photomultiplier tube and displayed on a storage oscilloscope. The efficiency of the sample was compared with microcrystalline powder of KDP and urea. The input energy used in this particular set-up is 2.2 mJ/pulse.

2.4. *Biological activity*

Antimicrobial activities of the compounds were tested *in vitro* by the well diffusion method [22] against bacteria *Escherichia coli* and *Bacillus subtilis* and yeast *Saccharomyces cerevisiae*. Chloramphenical was used as control. On the Muller Hinton agar plate, 0.1 mL of bacterial culture was inoculated and the well was prepared on a Muller Hinton agar plate using a cork borer. 10 µL of each compound (10 mmol L^{-1}) was placed in the plates, incubated at 30°C for 24 h, and observed for antibacterial activity. The activity was measured in terms of zone of inhibition.

Table 1. Analytical, molar conductance, and magnetic susceptibility data of HPIP and metal(II) complexes.

Compound	m.p. (°C)	Calculated (found), % M	C	H	N	Conductance ($S\,cm^2\,m^{-1}$)	μ_{eff} (BM)
HPIP	145	–	77.5(77.4)	4.94(4.92)	5.3(5.2)	–	–
$[CuLCl_2(H_2O)_2]$	240	14.5(14.2)	47.1(46.8)	3.92(3.90)	3.2(3.0)	26	1.96
$[CoLCl_2(H_2O)_2]$	280	13.7(13.5)	47.5(47.3)	3.96(3.90)	3.2(3.1)	23	4.71
$[NiLCl_2(H_2O)_2]$	209	13.6(13.2)	47.6(47.2)	3.97(3.93)	3.3(3.0)	3.9	3.20
$[ZnLCl_2(H_2O)_2]$	185	15.0(14.8)	46.8(46.4)	3.90(3.86)	3.2(2.9)	7.1	–
$[MnLCl_2(H_2O)_2]$	175	12.6(12.3)	46.8(46.5)	3.89(3.80)	3.1(2.9)	1.6	5.64
$[CdLCl_2(H_2O)_2]$	210	23.3(23.0)	42.3(42.0)	3.52(3.48)	2.9(2.5)	12.2	–
$[CuL_2(H_2O)_2]$	192	10.1(9.8)	65.5(65.0)	4.49(4.45)	4.5(4.4)	20	1.94
$[CoL_2(H_2O)_2]$	288	9.5(9.2)	65.9(65.6)	4.52(4.48)	4.5(4.3)	15	4.68
$[NiL_2(H_2O)_2]$	295	9.5(9.3)	65.9(65.3)	4.52(4.50)	4.5(4.2)	5.6	3.22
$[ZnL_2(H_2O)_2]$	204	10.4(10.0)	65.2(65.0)	4.47(4.43)	4.5(4.0)	8.9	–
$[VOL_2]SO_4$	223	7.4(7.0)	59.4(59.0)	4.07(4.00)	4.4(4.3)	6.3	1.81

2.5. *Gel electrophoresis*

Gel electrophoresis experiments were performed by incubation at 35°C for 2 h by taking 30 $\mu mol\,L^{-1}$ CT DNA, 50 $\mu mol\,L^{-1}$ solution of each complex, and 50 $\mu mol\,L^{-1} H_2O_2$ in 50 $mmol\,L^{-1}$ tris-HCl buffer (pH 7.2). The samples were electrophoresed for 2 h at 50 V on 1% agarose gel using a tris-acetic acid –EDTA buffer, pH 7.2, and the gel was stained using 1 $\mu g\,cm^{-3}$ ethidium bromide (EB) and photographed under UV-light.

3. Results and discussion

The analytical data and physical properties of HPIP and metal(II) complexes are presented in table 1. The molar conductances imply that all the complexes are non-electrolytes. Analytical data of the complexes are in good agreement with the general formula $[MLX \cdot 2H_2O]$ for Cu(II), Ni(II), Co(II), Zn(II), Mn(II), Cd(II) where $X = 2Cl^-$; $[ML_2 \cdot 2H_2O]$ for Cu(II), Ni(II), Co(II), Zn(II), and $[ML_2]X$ for VO(II) where $X = SO_4^{2-}$. The magnetic moments of the complexes are consistent with octahedral geometry around metal(II); the VO(II) complex exhibits square-pyramidal geometry.

3.1. *NMR spectra*

In comparison with ^{1}H-NMR spectrum of HPIP, zinc(II) complex confirms that –OH proton (13.25 δ in ligand) is present in the complex, shifted downfield (13.35 δ), suggesting deshielding of the hydroxyl group due to coordination. The signal at 4.95 δ shows the presence of water [23]. There is no appreciable change in other signals of this complex.

3.2. *IR spectra*

HPIP shows a broad band at 3150 cm^{-1} (table 2), which is characteristic of the hydroxyl group which is shifted to lower frequency (3109–3050 cm^{-1}) in complexation supporting

Table 2. IR spectral data (in cm^{-1}) of HPIP and complexes.

Compound	ν(O–H)	ν(OH) (H_2O)	ν(C=O)	ν(C=C)	ν(C–O)(phenol)
HPIP	3150	–	1631	1533	1315
$[CuLCl_2(H_2O)_2]$	3062	3292	1620	1567	1327
$[CoLCl_2(H_2O)_2]$	3050	3294	1600	1543	1342
$[NiLCl_2(H_2O)_2]$	3078	3310	1602	1543	1342
$[ZnLCl_2(H_2O)_2]$	3053	3294	1635	1544	1343
$[MnLCl_2(H_2O)_2]$	3055	3295	1627	1546	1341
$[CdLCl_2(H_2O)_2]$	3109	3371	1609	1550	1373
$[CuL_2(H_2O)_2]$	3060	3309	1598	1547	1365
$[CoL_2(H_2O)_2]$	3051	3345	1611	1573	1342
$[NiL_2(H_2O)_2]$	3054	3394	1609	1557	1366
$[ZnL_2(H_2O)_2]$	3100	3300	1626	1573	1343

coordination of hydroxyl oxygen [24]. The band at 1631 cm^{-1} from keto is shifted to 1627–1598 cm^{-1} in complexes implying coordination of carbonyl oxygen to the metal. The band at 1315 cm^{-1} is characteristic for phenolic ν(C–O). This band shifts to 1327–1373 cm^{-1} in all the complexes, due to chelation of phenolic oxygen to metal. The new band at 410–460 cm^{-1} is attributed to ν(M–O) [25]. The broad band due to ν(NH) in the indole ring of the ligand at 2924 cm^{-1} is not changed in spectra of complexes, indicating that the above group is not involved in coordination. In the vanadyl complex, a new band at 995 cm^{-1} is attributed to ν(V=O). Coordinated water in the complexes is confirmed by a broad band at 3400 cm^{-1} and a weak band around 825 cm^{-1}, indicating the binding of water to the metal [26, 27].

3.3. *Electronic spectra*

Electronic absorption spectral data (cm^{-1}) of HPIP and complexes in DMSO are given in table 3. The UV-Vis spectrum [ML] of the copper(II) complex shows three bands, assigned as an intraligand charge transfer (INCT) at 24,095 cm^{-1}, ligand-to-metal charge transfer (LMCT) at 22,172 cm^{-1}, and a d–d band at 11,876 cm^{-1} due to $^2E_g \rightarrow {}^2T_{2g}$ [28]. This relatively low-energy broad band indicates splitting of the E_g level caused by Jahn–Teller distortion in octahedral geometry; this is further supported by the magnetic susceptibility value (1.96 BM). The nickel(II) complex exhibits three d–d bands [29] at 9727, 13,440, and 24,096 cm^{-1}, assigned to $^3A_{2g} \rightarrow {}^3T_{2g}$, $^3A_{2g} \rightarrow {}^3T_{1g}(F)$, and $^3A_{2g} \rightarrow {}^3T_{1g}(P)$, respectively. The magnetic moment of Ni(II) complex is 3.20 BM, characteristic of two unpaired electrons from an octahedral geometry. The cobalt(II) complex indicates three absorption bands [30] at 9569, 16,260, and 21,413 cm^{-1}, tentatively assigned as $^4T_{1g}(F) \rightarrow {}^4T_{2g}(F)$, $^4T_{1g}(F) \rightarrow {}^4A_{2g}(F)$, and $^4T_{1g}(F) \rightarrow {}^4T_{1g}(P)$, respectively. The band at 9569 cm^{-1} is characteristic of distorted octahedral geometry, also supported by its magnetic susceptibility value (4.71 BM). The Mn(II) complex shows bands at 10,090, 23,148, and 27,310 cm^{-1}, assignable to $^4T_{1g} \rightarrow {}^6A_{1g}$, $^4T_{2g}(G) \rightarrow {}^6A_{1g}$, and $^4T_{1g}(D) \rightarrow {}^6A_{1g}$ transitions, respectively [31]. The magnetic moment value of 5.64 BM corresponds to five unpaired electrons, indicating octahedral Mn(II).

In the electronic spectrum of $[CuL_2]$, the observed transitions are at 11,904 cm^{-1} for $^2E_g \rightarrow {}^2T_{2g}$, which indicates splitting of the E_g level caused by Jahn–Teller distortion

Table 3. Electronic spectral data (cm^{-1}) of metal(II) complexes.

Compound	Frequency (ε) cm^{-1}	Assignment	Geometry
$[CuLCl_2(H_2O)_2]$	24,095 (3116)	INCT	Distorted octahedral
	22,172 (2273)	INCT	
	11,876 (1206)	$^2E_g \rightarrow {}^2T_{2g}$	
$[CoLCl_2(H_2O)_2]$	9569 (250)	$^4T_{1g}(F) \rightarrow {}^4T_{2g}(F)$	Distorted octahedral
	16,260 (720)	$^4T_{1g} \rightarrow {}^4A_{2g}$	
	21,413 (1364)	$^4T_{1g}(F) \rightarrow {}^4T_{1g}(P)$	
$[NiLCl_2(H_2O)_2]$	9727 (370)	$^3A_{2g} \rightarrow {}^3T_{2g}$	Distorted octahedral
	13,440 (970)	$^3A_{2g} \rightarrow {}^3T_{1g}(F)$	
	24,096 (1667)	$^3A_{2g} \rightarrow {}^3T_{1g}(P)$	
$[CuL_2(H_2O)_2]$	19,407 (1614)	INCT	Distorted octahedral
	11,904 (450)	$^2E_g \rightarrow {}^2T_{2g}$	
$[CoL_2(H_2O)_2]$	9784 (150)	$^4T_{1g}(F) \rightarrow {}^4T_{2g}(F)$	Distorted octahedral
	14,705 (540)	$^4T_{1g} \rightarrow {}^4A_{2g}$	
	20,703 (2014)	$^4T_{1g}(F) \rightarrow {}^4T_{1g}(P)$	
$[NiL_2(H_2O)_2]$	9756 (370)	$^3A_{2g} \rightarrow {}^3T_{2g}$	Distorted octahedral
	13,333 (175)	$^3A_{2g} \rightarrow {}^3T_{1g}(F)$	
	20,576 (1667)	$^3A_{2g} \rightarrow {}^3T_{1g}(P)$	
$[VOL]SO_4$	12,269 (185)	$^2B_2 \rightarrow {}^2E$	Square pyramidal
	20,283 (2023)	$^2B_2 \rightarrow {}^2B_1$	
	24,096 (3038)	$^2B_2 \rightarrow {}^2A_1$	

Table 4. Redox potential for copper(II) complexes.

Complex	E_{pc} (V)	E_{pa} (V)	I_{pc} (μA)	I_{pa} (μA)
$[CuLCl_2(H_2O)_2]$	0.129	0.375	6.499	4.686
$[CuL_2(H_2O)_2]$	0.090	0.351	7.450	6.626

in octahedral geometry, also shown by the magnetic moment of 1.94 BM [28]. The nickel(II) complex exhibits three d–d bands [29] at 9756, 13,333, and 20,576 cm^{-1}, assigned to $^3A_{2g} \rightarrow {}^3T_{2g}$, $^3A_{2g} \rightarrow {}^3T_{1g}(F)$, and $^3A_{2g} \rightarrow {}^3T_{1g}(P)$, respectively. The magnetic moment of Ni(II) complex is 3.22 BM, characteristic of an octahedral geometry. The cobalt(II) complex displays three absorptions [30] at 9784, 14,705, and 20,703 cm^{-1}, which are assigned as $^4T_{1g}(F) \rightarrow {}^4T_{2g}(F)$, $^4T_{1g}(F) \rightarrow {}^4A_{2g}(F)$, and $^4T_{1g}(F) \rightarrow {}^4T_{1g}(P)$, respectively. The band at 9784 cm^{-1} confirms octahedral geometry, which is also confirmed by its magnetic moment of 4.68 BM. For the vanadyl(II) complex, three bands at 12,269, 20,283, and 24,096 cm^{-1} are assigned to $^2B_2 \rightarrow {}^2E$, $^2B_2 \rightarrow {}^2B_1$, and $^2B_2 \rightarrow {}^2A_1$ transitions, respectively. From the band at 12,269 cm^{-1}, a square pyramidal geometry is proposed for vanadyl(II) complex; the geometry is further confirmed by its magnetic moment of 1.81 BM [32].

3.4. *Electrochemical behavior*

The redox behaviors of the copper(II) and oxovanadium(II) complexes were studied using CV at 10^{-3} mol L^{-1} in DMSO (table 4). The CV data of the copper(II) complexes show one reduction peak for Cu(II) → Cu(0) in cathodic side and for Cu(0) → Cu(II)

Table 5. The spin Hamiltonian parameters of copper(II) complexes.

Complex	A_{iso}	g_{iso}	$g_{\|\|}$	$g_{\perp}$	$A_{\|\|}$	$A_{\perp}$	α^2	β^2	$g_{\|\|}/A_{\|\|}$
		(10^{-4}cm^{-1})				(10^{-4}cm^{-1})			(cm)
$[CuLCl_2(H_2O)_2]$	109	2.293	2.31	2.24	136.4	134.4	0.38	3.02	169
$[CuL_2(H_2O)_2]$	137	2.292	2.32	2.21	87.8	112.6	0.24	3.73	269

Table 6. Fluorescence parameters of HPIP and its metal complexes in DMSO.

Compound	Emission $\lambda_{\max}$ (nm)	Excitation $\lambda_{\max}$ (nm)
HPIP	414	415
$[CuLCl_2(H_2O)_2]$	451, 551	546
$[CoLCl_2(H_2O)_2]$	541	532, 493
$[NiLCl_2(H_2O)_2]$	510	508
$[CuL_2(H_2O)_2]$	584	533
$[CoL_2(H_2O)_2]$	540	532
$[NiL_2(H_2O)_2]$	490	487
$[VOL_2]SO_4$	509, 598	440, 492

in anodic side. The peak current for the complex varies with scan rates and the $E_{\text{pa}}-E_{\text{pc}}$ values are greater than 200 mV, which indicates that the reductions are irreversible [33]. The oxovanadium complex exhibited two reduction peaks [34] at 0.620 and 0.341 V and one oxidation peak at 0.0198 V. The redox process involved is $V(IV) \rightarrow V(III) \rightarrow V(II) \rightarrow V(IV)$.

3.5. *EPR spectra*

EPR spectra of copper(II) complexes were recorded in DMSO at 300 and 77 K and the spin Hamiltonian parameters of the complexes are listed in table 5. The observed spectral parameters show $g_{||} > g_{\perp}$, characteristic of an axially elongated octahedral geometry [35]. The g_{iso} value is almost 2.3, indicating the covalent character of the metal ligand bond. The unpaired electrons lie predominantly in the $d_{x^2-y^2}$ orbital, evident from the value of the exchange interaction term G. The observed value of $G < 4$ for copper(II) complexes suggest that the exchange coupling is present and misalignment is appreciable. The α^2 value indicates appreciable in-plane covalency in the bonding. The calculated $(g_{||}/A_{||})$ value for the complexes indicates that the geometry is strongly distorted octahedral. The orbital reduction factors $K_{||}$ and $K_{\perp}$ [36] with $K_{||}$ (1.02) $> K_{\perp}$ (0.66) indicates poor in-plane π bonding which is also reflected in β^2 values.

3.6. *Fluorescence*

HPIP displayed an emission band at 414 nm in DMSO upon photoexcitation at 415 nm. The Cu(II), Co(II), Ni(II), and VO(II) complexes of both [ML] and $[ML_2]$ also exhibit emission bands around 490–598 nm and 440–546 nm on photoexcitation (table 6).

In general, fused ring systems such as indole and its derivatives exhibit fluorescence emission in the above region. In the same way, the free ligand and its metal complexes show an enhanced fluorescent intensity. This emission is neither metal-to-ligand charge transfer (MLCT) nor LMCT in nature. A lone pair of electron on oxygen and on carbonyl chromophore can quench the fluorescence of the indole moiety through photoinduced electron transfer. This leads to draining out of these pairs of electrons onto the metal orbital *via* complex formation causing a suppression of this fluorescence quenching. The above process is responsible for increase in fluorescence intensity [37].

3.7. *NLO property*

SHG efficiency measurements clearly reveal that HPIP is 30 times more active than that of urea and 120 times more active than KDP. This efficiency is higher than that reported for structurally related compounds [38, 39].

3.8. *Biological activity*

Zones of inhibition of the investigated compounds against the bacteria are summarized in table 7. The observed values indicate that most of the complexes have higher activity than the free ligand. Such an increased activity of the complexes can be explained on the basis of chelation theory [40, 41] and size of the metal ion. Muthukumar and Viswanathamurthi [42] investigated antifungal activity of chalcone complexes with reference to Bavistin as antifungal standard drug. Another type of chalcone complex reported by Zoldakova *et al*. [43] exhibited high inhibiting behavior to the cancer cell growth than respective chalcone. Prajapati *et al*. [44] reported cytotoxicity on Dalton lymphoma cell lines of a chalcone complex. In this study, though, chalcone and its complexes possess antibacterial activity; they are not effective to the standard drug Chloramphenical. This variation depends either on the impermeability of the cells of the microbes or differences in ribosome of microbial cells.

Table 7. Antimicrobial activity of HPIP and its metal complexes (zones of inhibition: diameters in cm**).

Compound	*B. subtilis*	*E. coli*	*S. cerevisiae*
HPIP	–	0.14	0.07
$[CuLCl_2(H_2O)_2]$	0.02	0.16	0.08
$[CoLCl_2(H_2O)_2]$	0.04	0.15	0.06
$[NiLCl_2(H_2O)_2]$	–	0.14	0.07
$[ZnLCl_2(H_2O)_2]$	–	0.13	0.06
$[MnLCl_2(H_2O)_2]$	0.04	0.12	0.07
$[CdLCl_2(H_2O)_2]$	0.03	0.14	–
$[CuL_2(H_2O)_2]$	0.05	0.17	0.08
$[CoL_2(H_2O)_2]$	0.04	0.16	0.07
$[NiL_2(H_2O)_2]$	–	–	0.06
$[ZnL_2(H_2O)_2]$	–	0.02	0.03
$[VOL_2]SO_4$	0.06	0.16	0.08
Chloramphenical	0.15	0.43	0.23

**Its value observed is within the error limits of ±0.02.

3.9. *DNA study*

CT-DNA electrophoresis for metal(II) complexes exhibits nuclease activity in the presence of H_2O_2. Control experiment using DNA alone (Supplementary material) does not show any significant cleavage of CT-DNA by H_2O_2. The cleavage efficiency of these complexes has been studied by comparing with their DNA-binding ability. The metal complexes are capable of converting super-coiled DNA into open circular DNA. The general oxidative mechanism is proposed for DNA cleavage by hydroxyl radicals *via* abstraction of hydrogen atom from sugar units. Several DNA cleavage studies of chalcone [45] have been reported, but so far to the best of our knowledge no work has been reported on chalcone metal complexes. Our investigation on copper(II) [ML_2] and cobalt(II) complexes of chalcone shows more cleavage against CT-DNA in the presence of H_2O_2 than other complexes, probably due to the redox couple of the metal ions. The above complexes may promote redox-mediated cleavage of DNA on the sugar ring.

4. Conclusion

The chalcone complexes [ML] and [ML_2] of Cu(II), Co(II), Ni(II), Zn(II), Mn(II), Cd(II), and VO(II) obtained from HPIP were synthesized and characterized by spectral and analytical methods (figure 2). HPIP exhibits appreciable NLO property in comparison with urea and KDP; hence, the compound may be studied for optical sensing material. Metal chelates show better antimicrobial activity than the free ligand. The CT-DNA interaction with cobalt(II) complexes [ML_2] leads to DNA cleavage in the presence of H_2O_2. HPIP and its metal complexes are fluorescent.

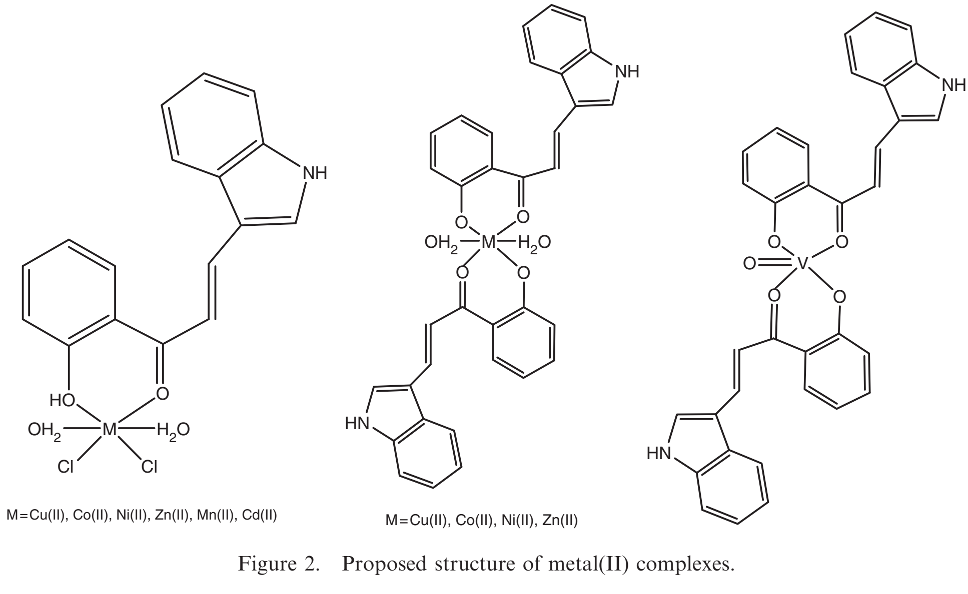

Figure 2. Proposed structure of metal(II) complexes.

Acknowledgments

The authors thank the Management of Thiagarajar College, Madurai, and one of the authors (PT) thanks the Defence Research and Development Organization (DRDO), New Delhi for providing financial support and SAIF, IIT, Bombay, and SAIF, CDRI, Lucknow for providing analytical facilities.

References

[1] S. Mukherjee, V. Kumar, A.K. Prasad, H.G. Raj, M.E. Bracke, C.E. Olsen, S.C. Jain, V.S. Parmar. *Bioorg. Med. Chem.*, **9**, 337 (2001).
[2] B.A. Bhat, K.L. Dhar. *Bioorg. Med. Chem. Lett.*, **15**, 3177 (2005).
[3] P. Boeck, C.A.B. Falcao, P.C. Leal, R.A. Yunes, V.C. Filho, E.C. Terres Santos, B. Rossi-Bergman. *Bioorg. Med. Chem.*, **14**, 1538 (2006).
[4] B.L. Wei, C.H. Teng. *Eur. J. Med. Chem.*, **42**, 660 (2007).
[5] S.N. Lopez, M.V. Castelli. *Bioorg. Med. Chem.*, **9**, 1999 (2001).
[6] Y.M. Lin, Y. Zhou, M.T. Flavin, L.M. Zhou, W. Nie, F.C. Chen. *Bioorg. Med. Chem.*, **8**, 2795 (2002).
[7] D.A.G.C. Pinto, A.M.S. Silva, J.A.S. Cavaleriro, J. Elguero. *Eur. J. Org. Chem.*, 747 (2003).
[8] N. Yayli, O. Ueuncu, E. Aydin, Y. Gok, A. Yasar, C. Baltaci, N. Yildirim, M. Kucuk. *J. Photochem.*, **169**, 228 (2004).
[9] M.E. Zwaagstra, H. Timmerman, M. Tamura, T. Tohma, Y. Wada, K. Onogi, M.Q. Zhang. *J. Med. Chem.*, **40**, 1075 (1997).
[10] R. Brouillard, O. Dangles, J.B. Harborne. *The Flavonoids: Advances in Research*, p. 565, Chapman & Hall, London (1986).
[11] Bhavana Sharma, S.C. Agrawal, K.C. Gupta. *Int. J. Chem. Res.*, **1** (2010).
[12] G.S. Gadaginamath, S.R. Pujar. *Indian J. Heterocycl. Chem.*, **11**, 207 (2002).
[13] B.H.M. Mruthyunjarwamy, B.K. Shanthaveerappa. *Indian J. Chem.*, **39B**, 433 (2000).
[14] P. Kant, R.K. Saksena, R. Yasmeen. *Indian Drugs*, **42**, 282 (2005).
[15] S. Dhar, D. Senapati, P.A.N. Reddy, P.K. Das, A.R. Chakravarty. *Chem. Commun.*, 2452 (2003).
[16] M.S. Ameerunisha Begum, S. Saha, A. Hussiain, A.R. Chakravarty. *Indian J. Chem.*, **48A**, 9 (2009).
[17] G. Saydam, H. Hakan Aydin, F. Sahin, O. Kucukoglu. *Leuk. Res.*, **27**, 57 (2003).
[18] W. Chen, Z. Yao, S. Ying, D. Liu, J. Liu. *J. Iran. Chem. Soc.*, **7**, 180 (2010).
[19] K. Rurack, J.L. Bricks, G. Reck, R. Radeglia, U. Resch Genger. *J. Phys. Chem.*, **104**, 3087 (2000).
[20] Z. Xu, G. Bai, C. Dong. *Bioorg. Med. Chem.*, **13**, 5694 (2005).
[21] S.K. Kurtz, T.T. Perry. *J. Appl. Phys.*, **39**, 3798 (1968).
[22] O.N. Irobi, M. Moo-Young, W.A. Anderson. *Int. J. Pharm.*, **34**, 87 (1996).
[23] M. Silverstein, X. Webster. *Spectrometric Identification of Organic Compounds*, 6th Edn, John Wiley & Sons, New York (2005).
[24] H. Keypour, S. Salehzadeh, R.V. Parish. *Molecules*, **7**, 140 (2002).
[25] N. Raman, L. Mitu, A. Sakthivel, M.S.S. Pandi. *J. Iran. Chem. Soc.*, **6**, 738 (2009).
[26] C.M. Sharaby. *Spectrochim. Acta*, **66**, 1271 (2007).
[27] A. Kulkarni, P.G. Avaji, G.B. Bagihalli, S.A. Patil, P.S. Badami. *J. Coord. Chem.*, **62**, 481 (2009).
[28] K.R. Reddy, K.M. Reddy, K.N. Mahendra. *Indian J. Chem.*, **45A**, 378 (2006).
[29] S. Chandra, D. Jain, A. Kumar Sharma, P. Sharma. *Molecules*, **14**, 174 (2009).
[30] M.M. Omar, G.G. Mohamed. *Spectrochim. Acta*, **61**, 929 (2005).
[31] G. Mohamed, M. Sharaby. *Spectrochim. Acta*, **66**, 949 (2007).
[32] R.C. Maurya, S. Rajput. *J. Mol. Struct.*, **24**, 794 (2006).
[33] R. Kannappan, R. Mahalakshmy, T.M. Rajendiran, R. Venkatesan, P. Sambasiva Rao. *Proc. Indian Acad. Chem. Sci.*, **115**, 1 (2003).
[34] A.B.P. Lever. *Inorganic Electronic Spectroscopy*, 2nd Edn, Elsevier, New York (1985).
[35] R.K. Ray, G.B. Kauffman. *Inorg. Chim. Acta*, **153**, 207 (1990).
[36] S.S. Dodwad, R.S. Dhamnasakar, P.S. Prabhu. *Polyhedron*, **8**, 1748 (1989).
[37] W. Wang, G. Springsteen, S. Gao, B. Wang. *Chem. Commun.*, 1283 (2000).
[38] V. Potheher, K. Rajarajan, M. Vimalan, T. Rajesh Kumar, R. Jeyasekaran, P. Sagayara. *Arch. Appl. Sci. Res.*, **2**, 171 (2010).
[39] M. Narayan Bhat, S.M. Dharmaprakash. *J. Cryst. Growth*, **242**, 245 (2002).
[40] P.B. Chakrawarthi. *J. Indian Chem. Soc.*, **78**, 273 (2001).

[41] C.D. Sheela, C. Anitha, P. Tharmaraj, D. Kodimunthri. *J. Coord. Chem.*, **63**, 884 (2010).
[42] M. Muthukumar, P. Viswanathamurthi. *J. Coord. Chem.*, **63**, 1263 (2010).
[43] M. Zoldakova, Z. Kornyei, A. Brown, B. Biersack, E. Madarász, R. Schobert. *Biochem. Pharmacol.*, **80**, 1487 (2010).
[44] R. Prajapati, S. Kumar Dubey, R. Gaur, R. Kumar Koiri, B. Kumar Maurya, S. Kumar Trigun, L. Mishra. *Polyhedron*, **29**, 1055 (2010).
[45] L. Dalla Via, O. Gia, G. Chiarelotto, M. Grazia Ferlin. *Eur. J. Med. Chem.*, **44**, 2854 (2009).